

Structural changes in the ageing periosteum using collagen III immuno-staining and chromium labelling as indicators

A. Al-Qtaitat^{1,2}, R.C. Shore³, J.E. Aaron¹

¹Faculty of Biological Sciences, University of Leeds, UK; ²Department of Anatomy and Histology, Faculty of Medicine, Muta'h University, Jordan; ³Oral Biology Unit, Dental Institute, University of Leeds, UK

Abstract

The periosteum and Sharpey's fibre extensions occupy the musculoskeletal interface and may be strategic in age-related deterioration. Because of its exceptionally powerful insertions the porcine mandible is an ideal model and its periosteal system was compared in 4 separate regions of adult young (1 year) and older (3 year) animals. These were examined by undecalcified histology, collagen immunohistochemistry and mineral histochemistry using polarization, epifluorescence and laser confocal microscopy; mineral ultrastructure was facilitated by chromium labelling with EDX microanalysis. Birefringent Sharpey's fibres were coarse (>8 µm) or fine and classified as horizontal (more common with age), oblique (most common in youth) or vertical (least common); in addition they were designated 'superficial', 'transcortical' and 'intertrabecular' (the latter being deep, coarse and vertical). Their specific affinity for collagen type III FITC-labelled antibody demonstrated 3-dimensional arrays of bone-permeating fibres. With age at each region the cortical thickness rose (e.g. 4.9 mm to 9.3 mm), the periosteum thinned (e.g. 180±7 µm to 129±8 µm; p<0.001), and the periosteum: bone ratio diminished (e.g. 3.65±0.36 to 1.40±0.14; p<0.001) while Sharpey's fibres became fewer, fragmented, superficial and shortened (e.g. 226±27 µm to 55±6 µm; p<0.001). Accompanying was the sporadic encroachment of calcified particles, 1 µm diameter, in irregular periosteal aggregates or interlinked around Sharpey bundles (resembling calcifying turkey leg tendon). EDX microanalysis confirmed prominent chromium spectral peaks in the older periosteum only, coincident with chromium-labelled mineral 'ghosts'. It was concluded that the periosteum and Sharpey's fibres, deep-penetrating and complex in youth, partially hardens and regresses with age with implications for its functional properties.

Keywords: Periosteum and Sharpey's Fibres, Musculoskeletal Exchange, Ageing Mandible, Collagen Type III Immunohistochemistry, Chromium Staining of Mineral "Ghosts"

Introduction

Histologically the periosteum consists of an outer fibrillar layer and an inner cellular layer containing osteoprogenitor cells. In the absence of active bone formation the fibrous layer becomes predominant and the inner layer poorly defined, although the few cells remaining are capable of mitosis and differentiation into osteoblasts should the need arise¹. The periosteum bonds to bone by means of its collagenous Sharpey's fibre extensions

which are also microscopic links between the exterior musculature and the interior skeleton. Although it is structurally unobtrusive, the function of the periosteal membrane cannot be overestimated since it has a primary role in the definition of bone developmental boundaries and in fracture repair, and its damage or absence can cause abnormality. At the same time, the Sharpey's fibres as anatomical extensions of the periosteum^{2,3}, ensure anchorage of the tendons and ligaments (themselves possibly modified periosteum⁴), as well as a scaffold for bone healing⁵ and their effectiveness will be governed by their penetration depth into the subperiosteal cortical bone. In particular these periosteal insertions which are well placed to serve also as avenues of musculoskeletal exchange are rich in collagen types III⁶ and VI⁷, in marked contrast to the surrounding matrix of collagen type I⁸. Their lack of calcification in young healthy bone means they are apparently resistant to osteoclastic resorption⁹, ensuring their stability and that of the bone they occupy. In this regard there is an extensive literature on the crucial nature of Sharpey's

The authors have no conflict of interest.

Corresponding author: Dr. Aiman Al-Qtaitat, Department of Anatomy and Histology, Faculty of Medicine, Muta'h University, B.O Box 2024, Karak, Jordan
E-mail: aimanaq2000@yahoo.com aimanaq@mutah.edu.jo

Edited by: D. Burr

Accepted 25 November 2009

Variables	Region			
	region3	region4	region5	region6
Young pig bone thickness μm	5420 \pm 102	4972 \pm 391	2152 \pm 40	4204 \pm 83
Old pig bone thickness μm	9645 \pm 31	9333 \pm 642	5791 \pm 22	6402 \pm 1750
<i>Young versus old bone thickness</i> <i>P</i> <	0.001	0.001	0.001	0.012
Young pig periosteum thickness μm	136 \pm 6	180 \pm 7	200 \pm 6	129 \pm 14
Old pig periosteum thickness μm	113 \pm 5	129 \pm 8	120 \pm 6	119 \pm 6
<i>Young versus old periosteum thickness</i> <i>P</i> <	0.001	0.001	0.001	0.132
Sharpey's fibre depth into young pig bone μm	139 \pm 8	226 \pm 27	197 \pm 9	148 \pm 10
Sharpey's fibre depth into old pig bone μm	101 \pm 3	55 \pm 6	128 \pm 6	125 \pm 4
<i>Young versus old Sharpey's fibre depth</i> <i>P</i> <	0.001	0.001	0.001	0.001
Young periosteum thickness to bone thickness ratio	2.51 \pm 0.09	3.65 \pm 0.36	9.29 \pm 0.24	3.07 \pm 0.30
Old periosteum thickness to bone thickness ratio	1.18 \pm 0.06	1.40 \pm 0.14	2.07 \pm 0.10	2.13 \pm 1.17
<i>Young versus old bone to periosteum ratio</i> <i>P</i> <	0.001	0.001	0.001	0.107

Table 1. Morphological comparison of the mandibular periosteum in younger and older adult pigs (Regions identified in Figure 1; mean \pm standard deviation).



Figure 1. The adult porcine mandible. Showing major sites of Sharpey's fibre insertions (shaded); numbered areas 1-5 indicate the buccal insertions and 6 is the lingual insertion.

fibres in the alveolar socket¹⁰⁻¹² where their central purpose as part of the periodontal ligament in tooth fixation is well recognized¹³⁻¹⁵, as are age-related changes, including progressive calcification¹⁶, that weaken their structural performance, thereby adversely affecting dentition. However, despite the oral significance of Sharpey's fibres any prime skeletal function they may have elsewhere has received little attention, although the tendons with which they integrate are reported to change from a pliant soft tissue as calcification advances to alter their mechanical properties¹⁷. Sometimes this is advantageous, as in the young

calcifying turkey leg tendon¹⁸, but perhaps as with teeth this is not always the case.

The aim of the following investigation was to select a skeletal location noted for exceptionally strong musculoskeletal interaction from which to determine any histological changes in the periosteal membrane in a young and older animal model. Particular attention was given to its periosteal Sharpey's fibre insertions and to i) their microanatomy, ii) their characteristic collagen type III immunostaining, iii) their histochemical and microanalytical calcification status and iv) their potential impact upon the structural 'quality' of the bone they occupy. The porcine mandibular bone fulfilled the criterion sought. However, because the density of its cortex means undecalcified microtomy/ultramicrotomy is technically demanding, sites of calcification were identified not only directly in undecalcified material but also indirectly in partially decalcified material using energy dispersive X-ray probe analysis (EDX) combined with a chromium label for the mineral "ghosts"^{19,20} as a novel application of an established method for the observation of calcification. The hypothesis to be tested using the porcine mandibular bone model is that the periosteum and its Sharpey's fibre extensions change organically and inorganically with age with implications for musculoskeletal exchange and bone structural "quality".

Materials and methods

Fresh sagittally hemi-sectioned adult skulls were obtained from a local abattoir from readily available young mature pigs about one year old (n 11), and from less readily available older

Periosteum and Sharpey's fibres

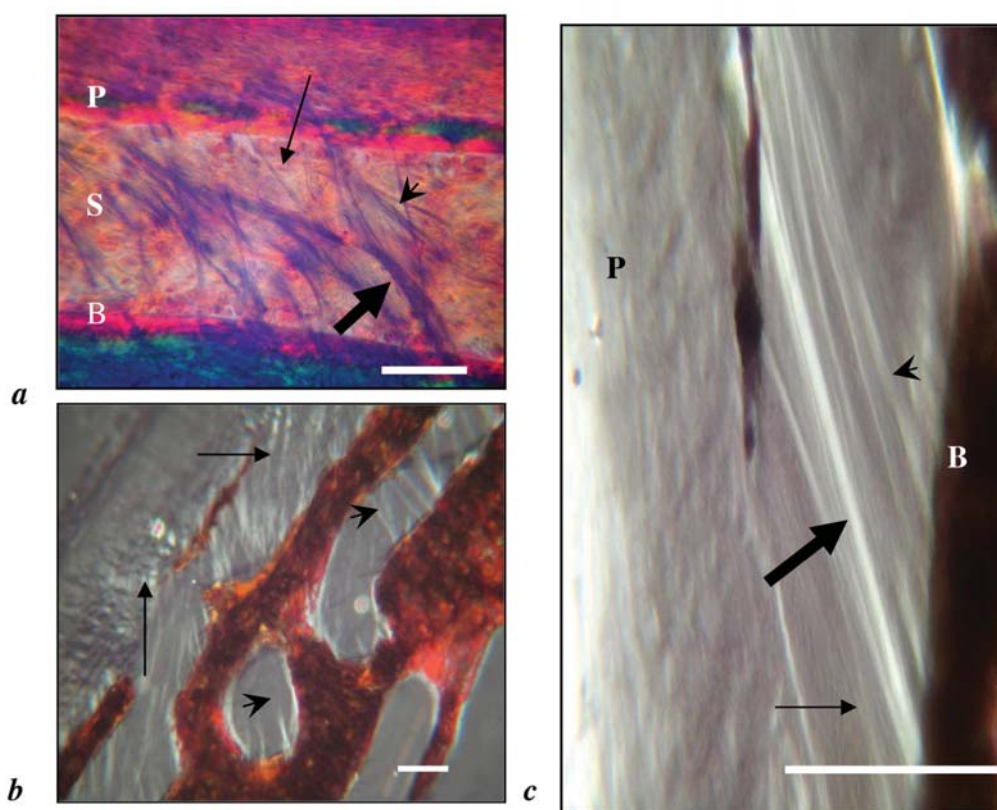


Figure 2. The periosteum typical of the young adult porcine mandible. Showing the periosteal membrane (P), Sharpey's fibres (S) and subperiosteal bone (B). a) Using the Goldner trichrome stain and polarized light; individual fine (small arrow) and coarse (arrowhead) birefringent fibre types and a prominent bundle of several fibres (large arrow), with most being oblique, some horizontal and a few vertical. b) Using the von Kossa stain and polarized light; intra- and sub-periosteal membrane fibres (small arrows) and intra-cortical fibres (arrowheads) are indicated and detailed in c) appearing as fine (small arrow), coarse (arrowhead) and bundled insertions (large arrow). Scale bar 50 μ m.

pigs (n 5) approximately three years of age. The porcine mandible was selected for attention because there is associated with it a more powerful musculature than at most other skeletal sites. The muscles were trimmed from the dissected mandible with a scalpel leaving only a small amount remaining and with care not to disrupt the periosteum. The mandibular bone was subdivided into segments relating to the muscle insertions, each sample being 2-4 cm x 2 cm (Figure 1).

Light microscopy of the periosteum

Using established undecalcified bone histology procedures²¹ some specimens were immediately preserved by immersion in 70% ethanol, followed by dehydration in graded concentrations of ethanol, 70%, 90%, 100%, for 24 hr in each followed by clearing in a mixture of ethanol and chloroform 1:1 for 24 hr, then xylene for 5 min. They were embedded undecalcified in methylmethacrylate by immersion in the monomer for 3 days, followed by immersion in the monomer containing 0.1% benzoyl peroxide catalyst for 3 days, followed by a final embedding

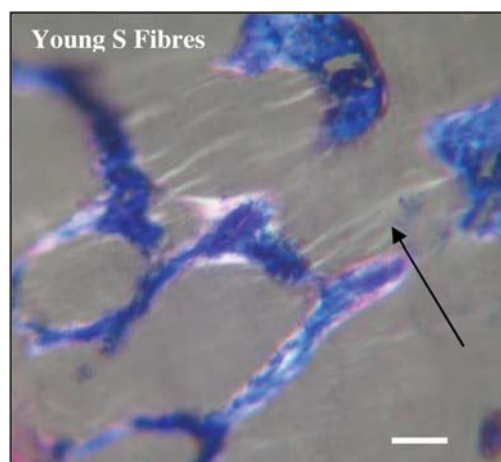


Figure 3. Deep-seated Sharpey's fibres in the young adult porcine mandible. Showing the Sharpey's fibres in parallel birefringent arrays (arrowed) traversing cancellous bone trabeculae and marrow spaces. Using the Masson trichrome stain and polarized light Scale bar 50 μ m.

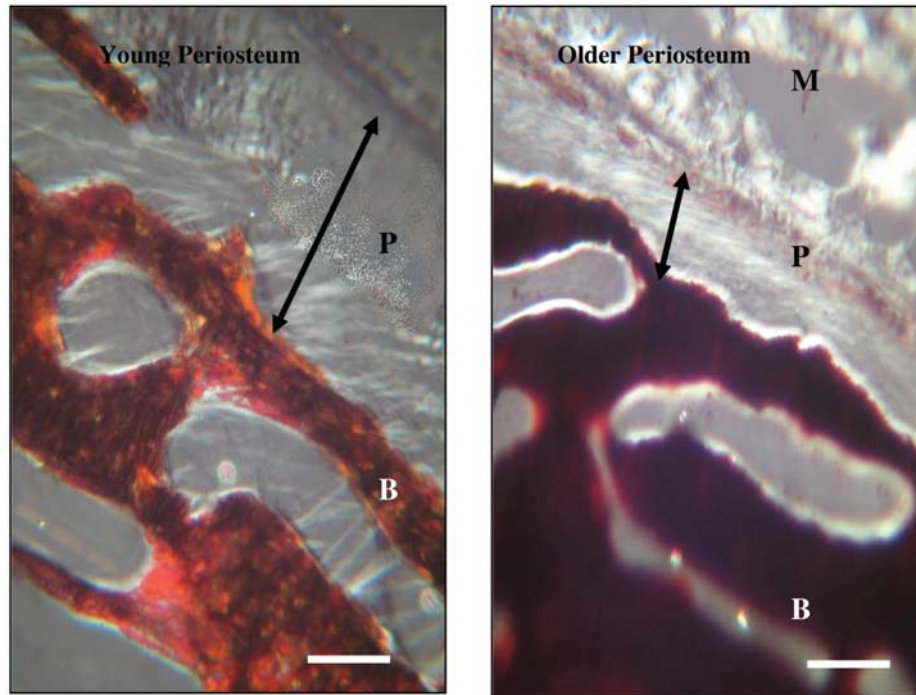


Figure 4. Comparison of the periosteum of young and older porcine mandible. Showing the periosteal membrane (P), bone (B) and muscle (M). Using the von Kossa stain and polarized light a diminution with time in the periosteal width (arrowed) and in the bone-penetration depth of the birefringent Sharpey's fibres is indicated, with more orientated horizontally than previously. (Also, not shown, the older periosteum stained more densely with the Masson trichrome stain for reasons not clear). Scale bar 50 μ m.

mixture of the monomer containing 2.5% benzoyl peroxide and 25% dibutylphthalate plasticizer. Polymerization took place in a water bath at 30°C²¹ and at no stage during processing did the pH fall below 7.5. Sections, 10 μ m thick, were cut on a Jung K heavy duty microtome (Reichert-Jung, Heidelberg). Representative sections were taken from the different surfaces of each block i.e. anteriorly, posteriorly, superiorly and inferiorly to enable the anatomical examination of Sharpey's fibres in all planes. The periosteum and Sharpey's fibres were stained histologically in Masson's trichrome stain, modified Goldner trichrome stain or toluidine blue stain (pH 7-9). They were also investigated histochemically for bone mineral using alizarin red stain for calcium, and von Kossa silver stain for phosphate/carbonate. In addition, specimens of calcifying turkey leg tendon, regularly used as a mineralization model^{22,23} were similarly prepared as above for a general comparison of their mineral pattern. Structural characteristics of the tissues were examined under a Zeiss Photomicroscope in plain light and also in polarised light since the collagenous Sharpey's fibres are birefringent^{5,7}. Measurements were made of the periosteal thickness and Sharpey's fibre penetration depth in the two porcine age groups as follows.

Histomorphometry: Using Goldner trichrome and Masson trichrome stained sections and a Zeiss calibrated eyepiece graticule, fifty fields from each region of the younger and older mandibles were scanned and measurements recorded of the periosteal thickness (between the lower muscle surface and the

upper bone surface), and the mandibular transverse width (from the outer subperiosteal surface to the inner one). In addition, the depth of Sharpey's fibre permeation (from the inner edge of the periosteum to the termination of the fibre (either naturally or artefactually by sectioning curtailment) was recorded for regions 3-6 (Figure 1). Mean values in each region were analysed for significant differences by the SPSS statistical package. In order to compare between means within a group and within groups we used analysis of variances (ANOVA test) in which the F test showed a significant results ($p < 0.05$) as shown in Table 1.

Immunohistochemistry of the periosteum

Fresh, frozen, undecalcified segments, 2 cm x 2 cm, were prepared for specific collagen type III immunofluorescence staining by snap-freezing intact in isopentane, cooling in liquid nitrogen, mounting in 1.6% carboxymethylcellulose gel, and storing at -30°C²⁴. Cryo-sections, 10-12 μ m thick, were cut on an LKB PMV 2258 heavy-duty cryomicrotome, after which they were thawed and fixed in cold formalin pH 7.2, demineralised to expose all epitopes in tetrasodium ethylenediamine tetracetic acid (EDTA), pH 7.0 for 3 min at room temperature²⁵ and washed three times for 5 min each in phosphate buffered saline (PBS), pH 7.2. Some sections were also pre-treated with bovine testicular hyaluronidase (Sigma, Poole, UK), 0.1 mg/1 ml PBS pH 7.2 for 20 min at 22°C, to expose any additional masked epitopes. Sections were incubated in anti-collagen type III primary anti-

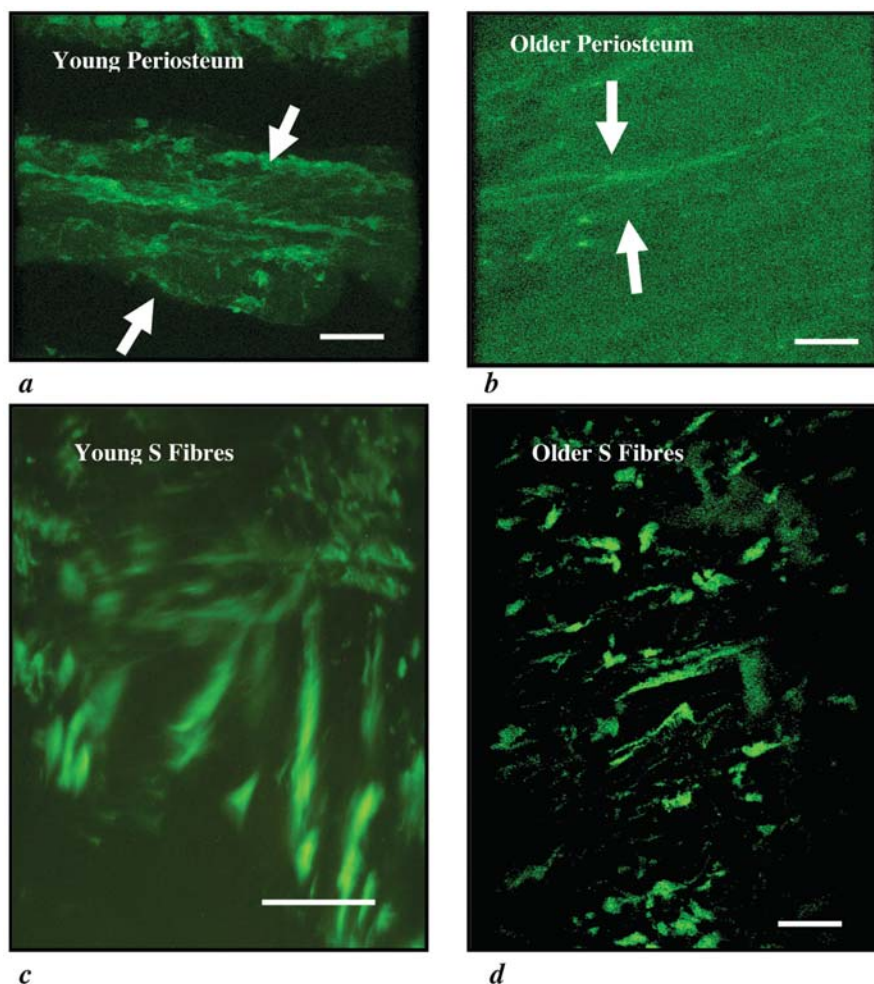


Figure 5. Comparison of the collagen type III immunostaining of the periosteum of young and older porcine mandible. Using confocal laser microscopy and FITC label showing a) and c) a wide, strongly fluorescent young adult periosteum (between arrows) rich in Sharpey's fibres (S Fibres; horizontal, vertical and oblique) and b) and d) a narrow weakly fluorescent older periosteum (between arrows) poor in Sharpey's fibres (mainly horizontal and fragmented). Scale bar 50 μm .

body, (mouse monoclonal; BioGenex, UK) which had been diluted 1:80 in PBS, pH 7.2 for 30 min in a dark humid chamber at 37°C, followed by further washing three times for 5 min each in PBS, pH 7.2. The secondary antibody was FITC-conjugated anti-mouse IgG (Sigma, UK) diluted 1:40 in PBS, pH 7.2 for 30 min in the dark humid chamber at 37°C. Stained sections were washed three times for 5 min each in PBS, pH 7.2 and mounted in the water-based mounting medium DABCO (0.25 g 1,4-diazobicyclo[2.2.2] octane; Sigma, Poole, UK, dissolved in 9 ml glycerol and 1 ml PBS, pH 7.2, corrected to pH 8.6 with N HCl) to avoid damage to the delicate sections by organic solvents and to optimally preserve the fluorescence from fading in ultraviolet light. As a control, some sections were incubated in PBS, pH 7.2, before immediate application of the FITC-conjugated secondary antibody i.e. without exposure to the primary antibody, to determine any non-specific tissue staining. Preparations were examined under a Nikon Eclipse E 400 epifluorescence microscope,

using ultraviolet light, and under a Leica TCS SP2 confocal laser scanning microscope (for the 3-D perspective), when positive regions should fluoresce an apple green colour.

Transmission electron microscopy (TEM) and EDX micro-analysis of the periosteum

Small segments 2x2 mm were taken from the angle and condylar regions 4 and 2 respectively (Figure 1), where prominent insertions were clear to the naked eye. Ultrathin periosteal sections were attempted, however, although the segments were tiny they proved difficult to cut even with a diamond-tipped knife fitted to the ultramicrotome because of the density of the cortex and its uneven hardness caused by the periosteal insertions. A solution for more intact ultrathin sections from this histologically challenging location was to use a comprehensive method of fixing, staining and also partially decalcifying in one single step by immersion in an aqueous solution of chromium sulphate $\text{Cr}_2(\text{SO}_4)_3$

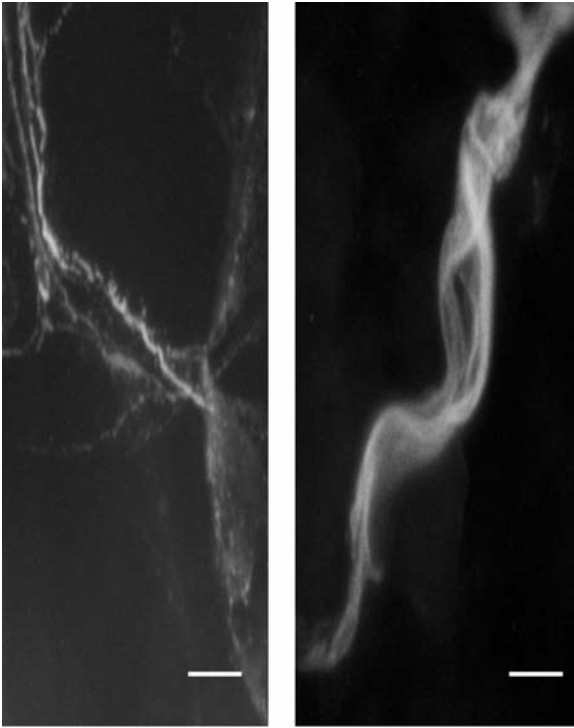


Figure 6. Collagen type III immunostaining of Sharpey's fibres in detail. Using confocal laser microscopy and FITC label showing a pair of composite fibre bundles; (*right*) a compact fibre bundle; (*left*) a dispersed fibre bundle terminating in a delicate fan-shaped array. Scale bar 25 μm .

$15\text{H}_2\text{O}$ (0.5% by weight which was allowed to stand for 2-3 days to complete dissolution) according to the technique of Appleton¹⁹ developed for the demonstration of organic mineral "ghosts". This method previously applied to cartilage²⁶ seems rarely to have been applied to bone even though removal of the mineral phase greatly facilitates ultramicrotomy, at the same time recording its distribution as a chromium-labelled "footprint". Specimens were placed in the chromium sulphate solution for three days at 37°C, followed by washing in distilled water, dehydration in ethanol, clearing in propylene oxide and embedding in epoxy resin. Semi-thin sections, 0.5 μm thick, were stained with toluidine blue for preliminary inspection and orientation. Ultrathin chromium sulphate-treated sections, 70-90 nm thick, were subsequently cut on a Leica Reichert Ultra-Cut microtome, floated from the water bath onto copper grids, air-dried and examined in a Philips TEM. Any electron dense crystal "ghosts" associated with the Sharpey's fibres, were subsequently confirmed by their chromium labelling signal registered by electron probe EDX microanalysis.

Results

Despite the cessation of growth in the younger animals, skeletal consolidation had continued for some time afterwards as indicated by the greater mandibular bone width of the older pigs in matched regions. The results (Table 1) confirmed that the mean periosteal

width was greater in the younger animals and also that the mean ratio of periosteum: bone width was larger in all regions. Similarly the penetration depth of the Sharpey's fibres in the young animal was greater than in the old. For example, in region 4 (Figure 1) where there were large muscle insertions Sharpey's fibre permeation was particularly great in the young animal whereas in the same region of the old animal it was notably less ($p < 0.001$). Thus even though its bone mass was greater, the thickness of the periosteum and the extent of its Sharpey's fibres was consistently less in the older pig than in its younger counterpart.

Light microscopy (LM) of the ageing periosteum: thickness, morphology

The two trichrome stains differentiated the mandibular periosteum, Sharpey's fibres and the underlying bone equally well, irrespective of age. Due to their strong birefringence, Sharpey's fibres were also identified within toluidine blue or von Kossa stained material using polarised light microscopy, and they were especially numerous and prominent in the angle and the coronoid process (Figure 1), where they formed the major part of the periosteum from which they extended inferiorly (Figure 2). Two types were distinguished, one coarse (8-25 μm thick) with a high trichrome staining affinity, and the other fine (<8 μm) with a low staining affinity. Their parallel arrays entered the subperiosteal bone in some cases almost horizontally (tangential fibres; especially common with age), in other cases perpendicularly (vertical fibres), but most commonly they were oblique (especially in the young). The horizontal insertions were expansive in areas of dense muscle attachment intermingling with the muscle fascicles to form a wide area of strong birefringence. The less common vertical fibres frequently traversed the cortex to the trabecular region and were generally of the coarse type either separate or mostly in bundles up to 40 μm thick. Thus, while many Sharpey's fibres apparently tapered with depth and terminated abruptly and superficially as is commonly described for Sharpey's fibres, others were deep-seated and transcortical, and in some instances even entered the medulla to become intertrabecular (Figure 3). The age-related changes in the periosteum are illustrated in Figure 4, where thinning was apparently accompanied by a diminution in the number, length and birefringence of its Sharpey's fibres, and where more randomly distributed and mainly superficial, horizontal insertions would provide truncated anchorage in the absence of the transcortical and intertrabecular fibres of youth.

Immunohistochemistry of the ageing periosteum: collagen type III

The periosteum stained positive for collagen type III as did also some parts of the endomysium, marrow reticular fibres and blood vessel walls. Fluorescent arrays of Sharpey's fibres contrasted with the negative bone matrix enabling their intraosseous pathways to be traced more clearly than above where they tended to be obscured by the matrix histological staining. The bright arrays were evident with both epi-fluorescence microscopy and confocal epi-fluorescence microscopy (Figure 5) and horizontal, oblique, and vertical insertions in some places appeared to constitute a

Calcifying Periosteum

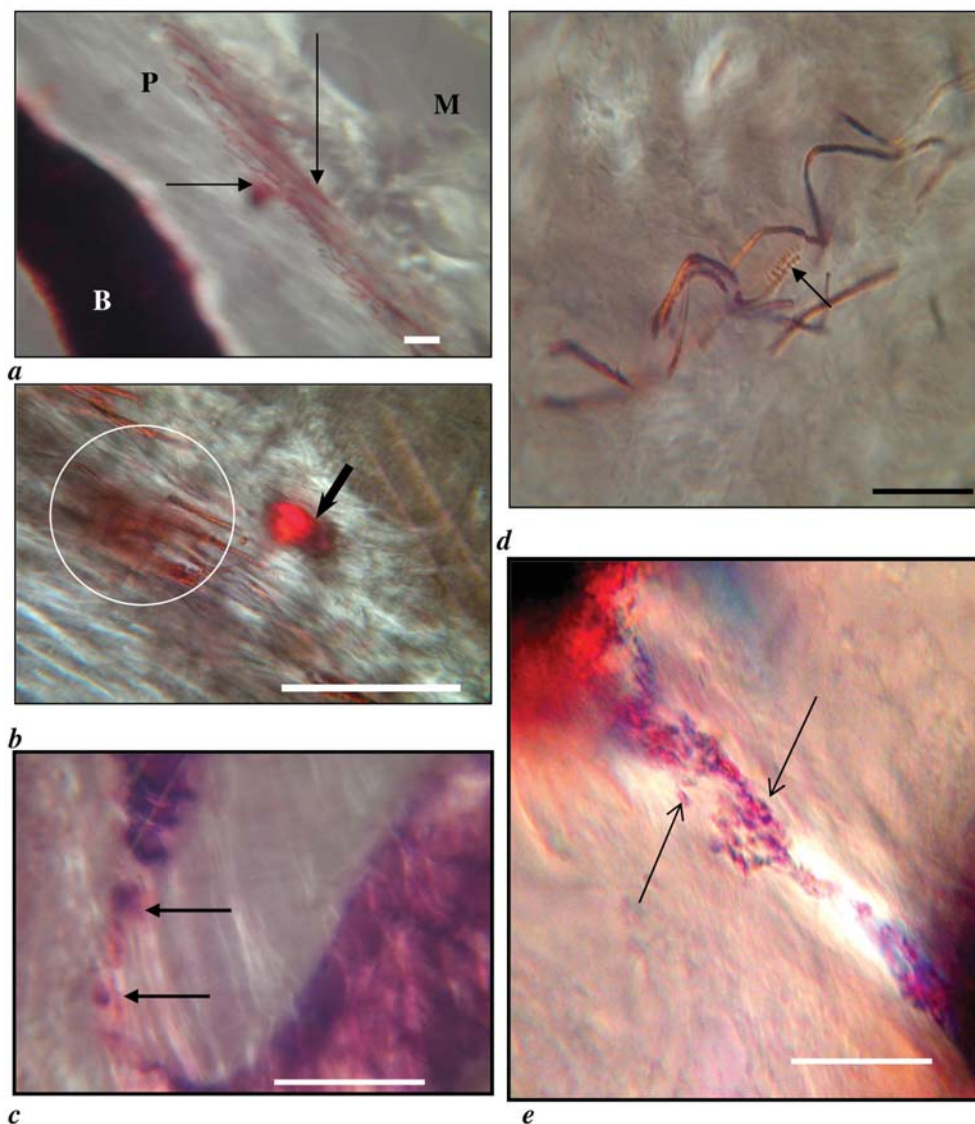


Figure 7. Calcification of the periosteum of the older porcine mandible. Showing the periosteum (P), bone (B) and muscle (M). Using optical histochemistry (plain and polarized light) with von Kossa and alizarin red stains for mineral. a) A group of horizontal calcified Sharpey's fibres (vertical arrow) and a small dense deposit (horizontal arrow) and b) in detail of a rectangular dense deposit (arrowed) and calcified Sharpey's fibres (encircled), von Kossa stain. c) A linear group of dense irregular periosteal deposits (arrowed), alizarin red stain. d) Convoluted calcified Sharpey's fibres beaded with chains of dense superficial particles (arrowed) and e) a coarse fibre bundle with assemblies of micron calcified particles (arrowed) along some of its length, von Kossa stain. Scale bar 50 μ m.

complex network-like structure apparently not previously recorded (Figure 6). In the older pig this mandibular subperiosteal domain containing the collagen III-stained Sharpey's fibres tended to fluoresce less well than in youth and apparently narrowed with age (Figure 5), such that parts of the matrix previously positive were now negative, cohorts of fibres that had been continuous seemed fragmented, and the insertions that had been typically multi-axial were weakly stained mainly horizontal and confined to limited parts of the of the periosteum only.

Mineral histochemistry of the ageing periosteum: LM, TEM, EDX, chromium labelling

Just as the periosteum apparently diminished with time, so also it became more susceptible to calcification, The histochemical stains for mineral indicated an affinity not only for the bone matrix but also sporadically for the periosteum and Sharpey's fibres in the older animal (Figure 7) and not evident in the younger one. The mineral deposits were in the form of small scattered discrete particles about 1 μ m in diameter resembling those compacted within

the calcified bone matrix^{9,21,27-29}. These occurred separately and in linear chains within parts of the periosteum and around some of the Sharpey's fibres as looped assemblies, an arrangement similar to the calcification pattern observed in the calcifying turkey leg tendon (Figure 8; see also³⁰). In addition were occasional larger, random, irregular dense aggregates, about 50 µm diameter, showing little structural alignment. The LM observations were recapitulated in more detail ultrastructurally (Figure 9). Associated with sites within the periosteal membrane and on the Sharpey's fibres of the older pig were electron dense labelled particles, approximately 1 µm in diameter, as chromium-stained mineral "ghosts"³¹, occurring separately and grouped into convoluted assemblies (Figure 9b). Each filamentous "ghost" had a beaded substructure of variable density²⁶ (Figure 9d). The micron chromium-labelled particles were rare or absent from the younger pig where any electron density (Figure 9a) was entirely confined to occasional clusters of small discrete objects, 50 nm in diameter, often with less dense centres, that may be precursors^{32,33}. Using chromium labelling in this way as an indirect marker of calcification the electron probe spectrum obtained from the mineral "ghosts" located among the Sharpey's fibres indicated that the elemental proportion of calcium, phosphate and chromium were all higher in the older pig than in the younger one where counts were low (Figure 9e-f). The presence of calcium and phosphorous peaks showed that the ultrathin sections were not completely decalcified at the ultrastructural level by chromium processing, even though no mineral could be resolved optically after such preparation.

Discussion

The evidence presented suggests that the periosteum as the intermediary between hard bone and soft muscle, is no less immune to the passage of time than are they. Periosteal Sharpey's fibres will be frequently subjected to tension in the direction of muscle pull and bone movement and their different axes will influence their capacity to dissipate these forces within the skeletal tissue. Just as Cohn (1972)^{34,35} related tooth movement to the realignment of Sharpey's fibres within the periodontal ligament, so Sharpey's fibres elsewhere may enable intraosseous stress modulation and accommodation. The transseptal fibres of the periodontal membrane are considered to be remnants of horizontal or oblique fibres from early development that have escaped the remodelling event³⁴, and four types were defined by Johnson (1987)³⁶. As such they may be analogous to the horizontal and oblique Sharpey's fibres above. At any given site Sharpey's fibres may be classified as a) fine or coarse, b) horizontal, oblique or vertical, and c) superficial, transcortical or intertrabecular, based on their histology. Functionally, it might be speculated that the superficial horizontal fibres have a role in propagating biomechanical exchange from the muscle across the periosteum, and that the short oblique transcortical fibres mediate exchange between the periosteum and outer cortex, additionally providing soft tissue anchorage. The long vertical intertrabecular fibres, on the other hand, with their uninterrupted course through the cortex and into trabeculae add a dimension of complexity concerning the muscle-

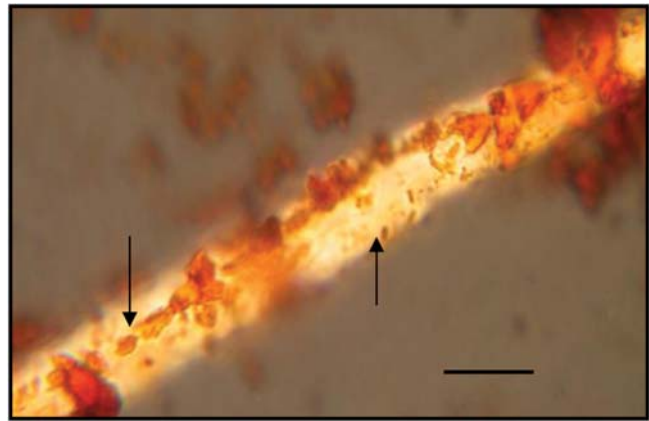


Figure 8. Calcification of an isolated fibre of turkey leg tendon for comparison with Figure 7e. Showing superficial assemblies of micron calcified particles (downward arrow) and individual particles (upward arrow) resembling those in the porcine periosteum. Von Kossa stain, polarized light. Scale bar 50 µm.

to-bone interface that may influence bone atrophy or augmentation and whether or not the region they permeate is sufficiently calcified to enable remodelling. Thus there is a strong similarity between the general pattern of Sharpey's fibre populations within the subperiosteal domain of the mandible and of collagen type III-rich fibres previously described in a subperiosteal domain in the proximal rat femur and responsive to both physical activity⁶ and oestrogen status⁷.

An elastic nature to his fibres was noted by Sharpey himself^{10,37} and contrasts markedly with the lack of elasticity and high tensile strength of tendon. This specific property of recoil must derive from their composite character which includes not only collagen type I³⁸ and elastin⁵ but also collagen type III, as well as collagen type VI which may add structural stability and discourage calcification⁷. An elastic nature would enable recovery after transient strain. Furthermore, the distal separation of coarse fibres into a delicate, finely dispersed fan that is apparent only with immuno-staining means they may be more functionally complex than previously supposed. Despite Sharpey's fibres being so uniquely placed to mediate musculoskeletal correlation and exchange, information about their calcification status is again apparently confined to their tooth-supporting role. In this capacity there are descriptions of alveolar Sharpey's fibres becoming partially calcified¹⁶, with age-related periodontal changes including fibrosis, increased cellularity and calcification³⁹⁻⁴¹, all contributing to a perceived degeneration. However, in the older pig (at this stage in its life by no means frail) the assemblies of interlinked mineral particles observed may increase the structural strength and binding together of the insertions, as is the case for the spindle-legged turkey; perhaps only in calcification excess are they compromised.

Although then, the pigs available for the investigation remain musculoskeletally competent throughout a confined domesti-

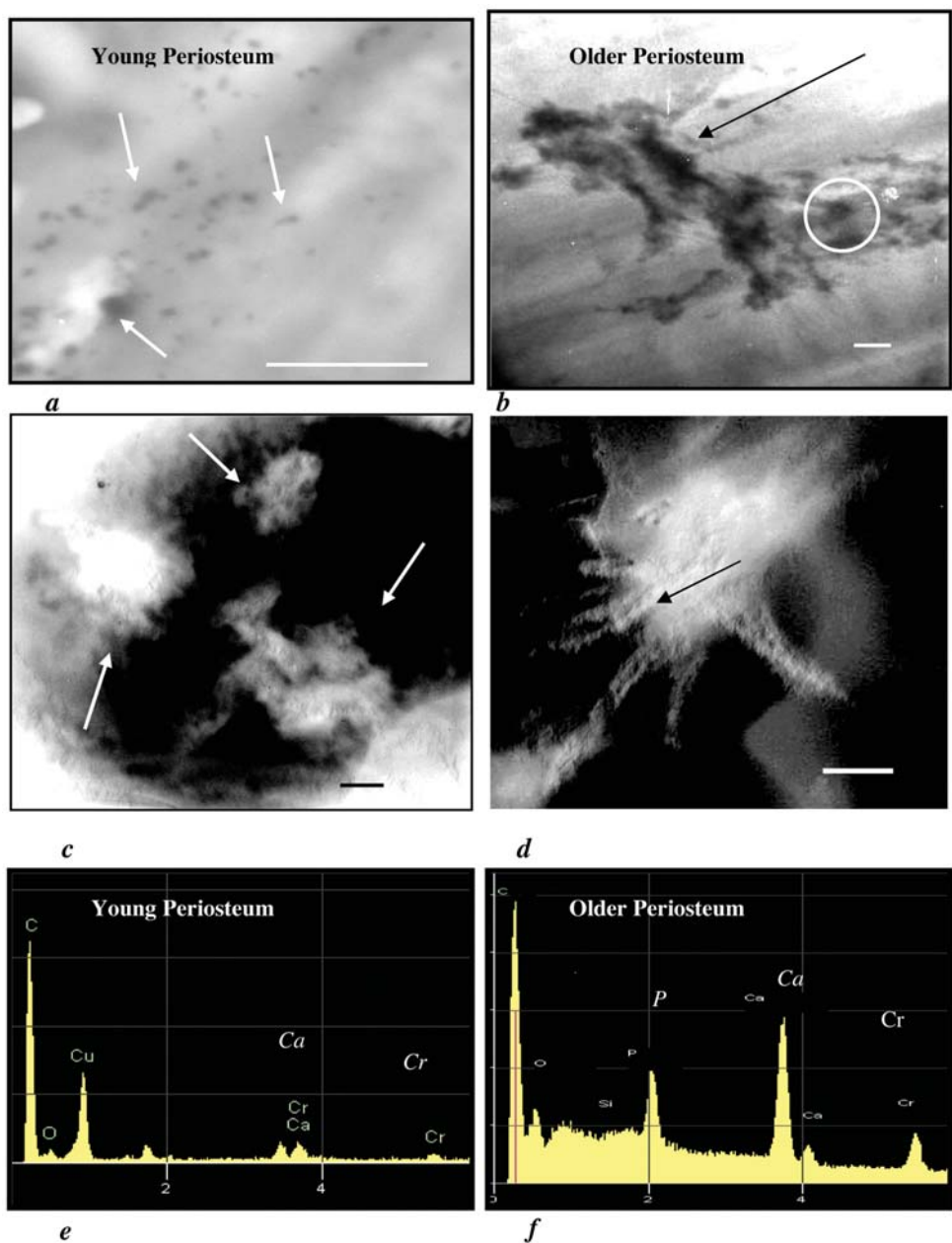


Figure 9. Comparison of the chromium labelling and EDX spectra of the periosteum of young and older porcine mandible. Showing partially decalcified mineral “ghosts”. Using chromium sulphate stain^{18,23} and ultrathin sections. a) Rare dispersed nanoparticles (arrowed) in the young periosteum in contrast to b) microparticles found individually (encircled) and grouped in bridged assemblies (arrowed) with age. Positive image (i.e. mineral dark), Scale bars 1 μm. c) Variable substructural density of three microparticulate clusters of mineral “ghosts” (arrowed), and d) a single microparticulate cluster of filamentous mineral ‘ghosts’ each filament resembling strings of beads (arrowed) and occasionally interlinked as binary chains. Negative image (i.e. mineral white). Scale bar 0.1 μm. (e-f) Corresponding periosteal EDX spectra in uncalcified youth showing a low Cr peak i.e. poor labelling, and in calcified age showing a high Cr peak i.e. prominent labelling.

cated life that rarely reaches its natural term, the question arises concerning any relevance the above periosteal phenomenon might have in the case of the elderly human. A correlation between the bone mass and muscle mass is widely recognized⁴², and physical exercise strengthens the skeleton by stimulating subperiosteal apposition (among other things), thereby incorpo-

rating into the cortex more Sharpey’s fibres as the bone front advances during lateral expansion, as is demonstrated in the voluntary running rat⁶. While muscles are resistant to calcification and they harden only in pathological conditions, tendons have been reported to calcify at their insertion into bone to increase their stiffness and to disperse and reduce the effect of stress at

the insertion site¹⁷. In their capacity as “micro-tendons” Sharpey’s fibre calcification may similarly reduce stress perception, and the calcification with age of the pliant young Sharpey’s fibres may buffer potentially damaging stress avoiding the detachment of the outer layer of the periosteum. In particular Leonard et al (1976)⁴³ showed that the tensile strength of the turkey leg tendon increases with age coincident with the onset of mineralization. Calcification of Sharpey’s fibres may similarly strengthen them especially if it is not random but is in the form of organized looped assemblies of bridged particles. Conversely, a decrease in extensibility and recoil may accompany the dense random irregular deposits sometimes observed among otherwise uncalcified fibres and reminiscent of the pathological condition calcifying tendonitis, where weakness is caused by accumulated mineral deposits which restrict movement.

Age-related mineralization of the Sharpey’s fibres seems to commence distally and to advance from the intraosseous depths out towards the periosteum. In excess it seems to be associated with the disappearance of the distal fine arrays such that the fibres appear shorter and eventually the periosteal membrane itself can be described as partially calcified^{45,46}. Since the periosteum is the developmental repository of skeletal form and function, it follows that its progressive hardening may be a factor in age-related skeletal incapacity. Chromium sulphate enables indirect visualization of the mineral in terms of the integral organic moiety of uncertain composition described by a number of authors as crystallite “ghosts”^{19,31}. The use of chromium stain in the present context is both novel and convenient (only one-step is needed, applied either *en bloc* or on sections) and by removing a proportion of the mineral the ultramicrotomy of the mature cortical bone is facilitated. This is essential as a larger block face can be cut than otherwise, thereby encompassing a more representative group of Sharpey’s fibres for analysis and not only an uncertain part of one as is the case within the limits of a typical tiny block face. The calcification of Sharpey’s fibres is identified ultrastructurally by the presence of crystallite “ghosts”. The relation between ghosts and crystallites is demonstrated when decalcification releases calcium salts leaving an organic framework previously masked by the morphology of the mineral. In the Sharpey’s fibres of youth, the rarity of the electron dense chromium stained mineral “ghosts” was confirmed by a barely registered chromium peak in the EDX spectrum relating to a few widely dispersed 50 nm objects³² in contrast to a prominent chromium peak with ageing and the accumulation of micron-sized clusters of filamentous “ghosts” and larger, irregular, dense aggregates. It might be argued that a difference in the stability rather than the amount of bone salt is an explanation for the ultrastructural distinction observed; indeed it is highly likely that the deposits in youth being “nascent” are readily removed. However, as the fixed organic mineral “footprint” is the index of change this cannot be the entire explanation. According to Jones and Boyde, (1974)⁴⁶ who wrote one of the few papers on the subject, the degree of mineralization of Sharpey’s fibres varies from mineralized periphery and an unmineralized core to a completely mineralised fibre.

Collagen type III as identified in the Sharpey’s fibres is abundant in embryonic tissues^{25,47} where it is involved in skeletal de-

velopment. With age, the fibroblasts differentiate to synthesise more collagen type I and less collagen type III^{48,49} such that the general proportion of collagen type III in old age is significantly less than in youth. At the same time, collagenase synthesis has been attributed to fibrocytes under certain conditions, and may be an intrinsic cause of fibre degeneration with time. A reduction of collagen type III associated with Sharpey’s fibres was observed with age in the pig model i.e. fewer uninterrupted, immuno-stained fibres with more calcified microspheres at their perimeter³⁰. While uncalcified Sharpey’s fibres may be protected from resorption since osteoclasts do not usually resorb uncalcified tissue^{27,28}, it follows that their progressive calcification may be counter-productive in so far as it risks removing that protection, enabling a remodelling advance that may loosen and destabilize the insertions. Populations of microspheres are skeletally prevalent and persistent^{29,50} and their encroachment with time into the soft fibrous periosteal system may be no more than a recapitulation of their normal interrelationship with the bone matrix and calcifying tendon^{22,51} to support an otherwise flexible structure in strategic places. Whether the periosteal mineral particles originated by migration from elsewhere⁵², arose in matrix vesicles^{28,53-56} or were synthesised by local fibroblasts-type cells³³ remains unclear. However, regular, uniform, needle-shaped crystals culminating from a random precipitation event were not a feature.

In conclusion, collagen III immunostaining extrapolates the histological ramifications of the periosteum into a structurally complex domain the delicate, fan-shaped outreaches of which disintegrate with time, with possible implications for musculoskeletal anchorage, exchange and multi-axial responsive function. The novel application to the periosteum of the ultrastructural chromium staining method for mineral “ghosts” supports the mineral histochemistry, and EDX microanalysis and spectral peaks confirm a progressive calcification event with age. Mineral microparticles transgress the discrete boundary of the hard tissues and invade the soft ones, to partially stiffen the periosteum together with its Sharpey’s fibre extensions, thereby destabilising and exposing to resorption prime areas of bone matrix previously protected by their presence. In this way the changing character of the periosteum with time may mean that its Sharpey’s fibres are as crucial to the retention of functioning bone within the musculature as they apparently are to the retention of functioning teeth within the gums.

Acknowledgements

The support for JA of Action Medical Research (PG AP1017) and the HSA Charitable Trust is gratefully acknowledged, as is also the postgraduate student anatomical sciences scholarship awarded to Dr A Al-Qtaitat by his sponsors Mu'tah University, Jordan. We are indebted to Dr DH Carter, University of Manchester for valuable discussion.

References

1. Ross MH, Kage GI, Pawlina W. Histology a Text and Atlas. Fourth edition. Maryland: Lippincott Williams and Wilkins, 2002.

2. Nordin M, Lorenz T, Campello M. Biomechanics of tendon and ligament. In Nordin M and Frankel VH editors. Basic Biomechanics of Musculoskeletal Systems pp 102-125. Maryland: Lippincott, Williams and Wilkins, 2002.
3. Weiner S and Wagner HD. The material bone: structure mechanical function relations. Annual Review of Material Sciences 1998;28:271-98.
4. Hurlle JM, Hinchcliffe JR, Ros MA, Critchlow MA, Genis-Galvez JM. The extracellular matrix architecture relating to myotendinous pattern formation in the distal part of the developing chick limb. Cell differentiation and development 1989;27:103-20.
5. Aaron JE, Skerry TM. Intramembranous trabecular generation in normal bone. Bone Mineral 1994;25:211-30.
6. Saino H, Luther F, Carter DH, Natali AJ, Turner DL, Shahataheri SM, Aaron JE. Evidence for an extensive collagen type III proximal domain in the rat femur. II. Expansion with exercise. Bone 2003;32:660-8.
7. Luther F, Saino H, Carter DH, Aaron JE. Evidence for an extensive collagen type III/VI proximal domain in the rat femur. I. Diminution with ovariectomy. Bone 2003; 32:652-9.
8. Smith JW. Collagen fibre pattern in mammalian bone. Journal of Anatomy 1960;94:329-44.
9. Aaron JE. Demineralization of bone *in vivo* and *in vitro* evidence of a microskeletal arrangement. Metabolic Bone Disease Related Research 1980;2S:117-25.
10. Black CV. Periosteum and periodontal membrane. Dental Review 1987;1:233-43.
11. Provenza DV. Oral Histology. Inheritance and Development. Lippincott, Philadelphia, 1964.
12. Tomes CS. A Manual of Dental Anatomy, Human and Comparative. Churchill: London, 1876; p. 89.
13. Barton JM, Keenan RM. The formation of Sharpey's fibres in the hamster under non-functional conditions. Archives of Oral Biology 1967;12:1331-6.
14. Bernick S, Levy BM, Driezen S, Grant DA. The interosseous orientation of the alveolar component of marmoset alveolodental fibres. Journal of Dental Research 1977;56:1409-16.
15. Johnson RB, Low FN. Development of transalveolar fibres in alveolar bone of the mouse. Archives of Oral Biology 1981;26:971-6.
16. Johnson RB. A new look at the mineralized and unmineralized components of intraosseous fibres of the interdental bone of the mouse. Anatomical Records 1983;206:1-9
17. Cooper RR, Misol S. Tendon and ligament insertion. A light and electron microscopy study. Journal of Bone and Joint Surgery 1970;52 A:1.
18. Colominas CB, Miller A, White SW. Structural study of the calcifying collagen in turkey leg tendon. Journal of Molecular Biology 1979;134:431-45.
19. Appleton J. Ultrastructure observation on early cartilage calcification, the use of chromium sulphate in decalcification. Calcified Tissue Research 1970;2:270-6.
20. Sundstrom B. A new technique for decalcifying thin ground specimen of adult human enamel. Archives of Oral Biology 1968;11:1221-23.
21. Aaron JE, Shore PA. Histomorphometry. In: The Physical Measurement of Bone. (CM Langton, CF Njeh, eds) Institute of Physics Publishing: Bristol, Philadelphia. 2004; p. 185-264.
22. Siperko LM and Landis WJ. Aspect of mineral structure in normal calcified avian tendon. Journal of Structural Biology 2001;135:313-20.
23. Colominas CB, Miller A, White SW. Structural study of the calcifying collagen in turkey leg tendon. Journal of Molecular Biology 1979;134:431-45.
24. Aaron JE, Carter DH. Rapid preparation of fresh frozen undecalcified bone for histological and histochemical analysis. Journal of Histochemistry and Cytochemistry 1987;35:361-9.
25. Carter D H, Sloan P, Aaron J E. Trabecular generation de novo: A morphological and immunohistochemical study of primary ossification in the human femoral anlagen. Anatomy and Embryology 1992;186:229-40.
26. Appleton J. Ultrastructure observation in the inorganic/organic relationships in early cartilage calcification. Calcified Tissue Research 1971;7:307-17.
27. Aaron JE. Histology and microanatomy of bone. In: Nordin, editor. Calcium, Phosphate and Magnesium Metabolism Edinburgh: Churchill, Livingstone, 1976; p. 298-356.
28. Aaron JE. Alkaline phosphatase, vesicles and calcification. Metabolic Bone Disease Related Research 1980; 2S:117-25.
29. Aaron JE. Bone turnover and microdamage. Advances in Osteoporotic Fracture Management 2003;2:4.
30. Al-Qtaitat AI. Anatomy of Sharpey's Fibres and their Calcification with Age. MSc Thesis, University of Leeds 2004.
31. Bonucci E. Fine structure of early cartilage calcification. Ultrastructure Research 1967;20:33-50.
32. Carter DH, Hatton PV, Aaron JE. The ultrastructure of slam-frozen bone mineral. Histochemical Journal 1997;29:783-93
33. Carter DH, Scully AJ, Davies RM, Aaron JE. Evidence of phosphoprotein microspheres in bone. Histochemical Journal 1998;30:677-86.
34. Cohn SA. A re-examination of Sharpey's fibres in alveolar bone of the mouse. Archives of the Oral Biology 1972; 17:255-60.
35. Cohn SA. A re-examination of Sharpey's fibres in alveolar bone of the marmoset. Archives of the Oral Biology 1972;17:261-9.
36. Johnson RB. A classification of Sharpey's fibres within the alveolar bone of the mouse: high voltage electron microscope study. Anatomical record 1987;217:339-47.
37. Sharpey W, Thompson A, Cleland J. Quain's Element of Anatomy 1867.
38. Tung PS, Domenicucci C Wasi S, Sodek J. Specific immunohistochemical localization of osteonectin and colla-

- gen I and III in fetal and adult porcine dental tissue. *Journal of Histochemistry and Cytochemistry* 1985; 33:531-40.
39. Quigley MB. Perforating (Sharpey's) fibres of the periodontal ligament and bone. *Journal of Medical Sciences* 1970;7:336-42.
 40. Shackelford JM. Microstructure and microradiographic characteristics of Sharpey's fibres in dog alveolar bone. *Journal of Medical Sciences* 1973;10:11-20.
 41. Sloan P, Carter DH, Kielty CM, Shuttleworth CA. An immunohistochemical study examining the role of collagen type VI in rodent periodontal ligament. *Histochemical Journal* 1993;25:523-30.
 42. Burr DB. Muscle strength, bone and age-related bone loss. *Journal of Bone and Mineral Research* 1997; 12:1547-51.
 43. Leonard F, Moscovitz J, Hodge JW, Adams JP. Age related Ca- Mg content and strength in turkey tendon. *Calcified Tissue Research* 1976;19:331-6.
 44. Zagba- Mongalima G, Goret-Nicaise M, Dhem A. Age changes in human bone: a microradiographic and histological study of subperiosteal and periosteal calcification. *Gerontology* 1988;34:264-76.
 45. Allen MR, Hock JM, Burr DB. Periosteum: biology, regulation and response to osteoporosis therapies. *Bone* 2004;35:1003-12
 46. Jones SJ, Boyde A. The organization and gross mineralization pattern of the collagen fibres in Sharpey's fibres bone. *Cell and Tissue Research* 1974;148:83-96.
 47. Carter DH, Sloan P, Aaron JE. Immunolocalization of collagen type I and III, tenascin and fibronectin in intramembranous bone. *Journal of Histochemistry and Cytochemistry* 1991;39:599-606.
 48. Keene DR, Sakai LY, Burgeson RE. Human bone may contain type III collagen type VI collagen and fibrillin: type III collagen may mediate attachment of tendons, ligament and periosteum. *Journal of Histochemistry and Cytochemistry* 1991;39:59-69.
 49. Tagasako T, Nakamura K, Kashiwagi S, Inoue SH, Oto H, Takeo K. Analysis of collagen type III between an uninterrupted sodium dodecyl sulphate polyacrylamide gel electrophoresis and immunoblotting: changes in collagen type III polymorphism in aging rats. *Electrophoresis* 1992;13:373-8.
 50. Aaron JE, Oliver B, Clarke N, Carter DH. Calcified microspheres as biological entities and their isolation from bone. *Histochemical Journal* 1999;31:455-70.
 51. Landis MJ, Hodgens KJ, Song MJ, Arena J, Kiyonaga S, Marko M, McEwen BF. Mineralization of collagen may occur on fibril surfaces. Evidence from conventional and high voltage EM and three dimensional imaging. *Journal of Structural Biology* 1996;117:24-35.
 52. Aaron JE. Osteocyte types in the developing mouse calvarium. *Calcified Tissue Research* 1973;12:259-79.
 53. Bonucci E. Further investigation of the organic/inorganic relationship in calcifying cartilage. *Calcified Tissue Research* 1968;3:38-54.
 54. Glimcher MJ, Krane SM. The organization and structure of bone and the mechanism of calcification. A treatise on collagen. *Biology of Collagen* 1968; IIB:68-251.
 55. Landis WJ, Arsenault L. Vesicle and collagen mediated calcification in turkey leg tendon. *Connective Tissue Research* 1989;22:35-42.
 56. Posner AS. Bone mineral and the mineralization process. *Bone and Mineral research* 1987;5:65-116.